WARSAW UNIVERSITY OF TECHNOLOGY Index 351733
FACULTY OF CIVIL ENGINEERING
COMMITTEE FOR CIVIL AND WATER ENGINEERING
POLISH ACADEMY OF SCIENCES ISSN 1230-2945
DOI: 10.24425/ace.2024.150990
ARCHIVES OF CIVIL ENGINEERING
Vol. LXX ISSUE 3 2024
pp. 387–400

Research paper

Evaluating methods for logging the pore structure of tight sandstone reservoir in Chang 6 member of the Yanchang Formation, Ordos Basin

Gaorun Zhong[1], Yajun Li[2], Yuhan Tan[3]

Abstract: Pore structure is a key parameter used to evaluate reservoir quality. At present, experimental method is the most important method to analyze reservoir pore structure. However, coring data may be limited, and it is not possible to perform experimental analyses on all cores. Therefore, the researchers explored the use of logging techniques to study the pore structure of reservoirs. The relationship between pore geometry index (PGI), pore permeability and mercury injection parameters was analyzed based on mercury injection experiment, thin slice analysis, production test data and well logging data. These results can then determine the response characteristics of the logging parameters that correspond to different pore structures and establish a method of modeling the PGI through a multiple parameter regression and neural network method. This research shows that: (1) PGI can quantitatively characterize pore structure, and the maximum pore throat radius, displacement pressure and flow unit index have the highest correlation with PGI, which can be accurately characterized by practical formulas; (2) Natural gamma ray, natural potential amplitude difference, acoustic transit time, density, compensated neutron, deep and shallow resistivity logging data can reflect the quality of the reservoir pore structure. However, there are limitations in evaluating reservoir pore structure with a single logging parameter. Multi-parameter regression method and neural network method realize the quantitative calculation of pore structure from the perspective of multi-parameter and nonlinear. (3) The neural network method and multiple parameter regression method are used to study the pore structure of reservoir and realize the continuous quantitative calculation of pore structure index in a single well. It can be used in uncored analysis Wells and as one of the parameters to evaluate reservoir pore structure.

Keywords: logging evaluation, multiparameter regression, neural network, pore structure, yanchang formation

[1]Ph.D., School of Petroleum Engineering and Environmental Engineering, Yan'an University, Yan'an 716000, China, e-mail: zhongaorun@126.com, ORCID: 0000-0002-3960-7702
[2]Ph.D., School of Petroleum Engineering and Environmental Engineering, Yan'an University, Yan'an 716000, China, e-mail: 251926279@qq.com, ORCID: 0000-0001-6768-7298
[3]MSc., CNLC Geology Research Institute, Xi'an 710077, China, e-mail: 390817824@qq.com, ORCID: 0000-0002-0809-1926

1. Introduction

In order to meet the needs of efficient oilfield development, the study of reservoir pore structures has been growing in importance. These studies have contributed to the formation of theoretical systems and technical methods such as experimental analysis, geophysical logging, mathematical statistics and numerical simulation. However, more attention will be given to studies that combine microscopic pore structure analyses with oil-bearing evaluations, oil and gas pressure mechanism analyses, and the optimization of reservoir development programs [1]. Reservoir pore structure analysis methods include high pressure mercury injection, constant velocity mercury injection, thin section analysis, scanning electron microscopy, CT scanning, nuclear magnetic resonance, gas adsorption, small Angle scattering and so on [2–4]. The gas adsorption method was used to characterize the nanoscale pores, and the adsorption status of CO_2 and CH_4 gases in the micropores was also investigated. X-ray and small-angle scattering methods are widely used in isolated pore testing [5–16]. Experimental techniques, such as large 2D backscattering image stitching technology, automatic mineral quantitative recognition systems, and multiscale micron CT scanning, have achieved the 2D and 3D multiscale fine characterization of low porosity and low permeability reservoirs [17]. Rich logging data provide basic conditions for characterizing reservoir microscopic pore structures. Based on various experimental analysis results, a logging model was established to quantitatively characterize pore structure by combining parameters such as mercury injection parameters, median pressure, and sorting coefficient with porosity, permeability, and logging parameters to continuously and quantitatively calculate reservoir microstructure parameters such as pore-throat size [18–22]. However, the structure derived from experimental analysis can be combined with geophysical well logging parameters through neural network and stepwise regression methods. This approach can be used to develop the logging evaluation model for the reservoir pore structure; thus achieving a continuous quantitative evaluation of the pore structure within a single well.

2. Materials and methods

In this experimental analysis, 67 samples from 46 Wells were selected for CT scanning, high pressure mercury injection and other related experimental analysis. Nine parameters such as porosity and permeability were obtained. Quantitative characterization of pore structure is the basis for accurate reservoir evaluation. Pore structure index (PGI) is defined as follows: PGI = maximum pore radius × maximum mercury saturation × mean pore radius × sorting coefficient ÷ displacement pressure.

The CT scanning core is light gray fluorescent fine sandstone, the sample diameter is 3.15 mm, the liquid porosity is 8.01%, the air permeability is 0.0837×10^{-3} μm^2, the analysis temperature is 23°, the matrix proportion is 94.1%, the connected porosity is 6.0%, the disconnected porosity is 1.4%, the heavy mineral proportion is 0.72%. The resolution is 1.5253 μm.

Capillary pressure curve of rock was measured, core diameter was 1.5 inches, length was 2.0 inches, analysis temperature was 25°, ambient pressure was 96.8 kPa, analysis was based on SY/T

5346-2005. The displacement pressure, median pressure, median radius of pore throat, mercury saturation, sorting coefficient, coefficient of variation and mercury removal efficiency were obtained.

Core physical property analysis mainly uses the instruments of Core Laboratory Company in the United States to measure porosity and permeability. The analysis temperature is 25°, the pressure is 1 atmosphere, the core diameter is 25 mm, the length is 45 mm.

3. Results and discussion

3.1. Thin section analysis results

In this study, 50 samples from 30 core wells were selected for thin section analysis. The primary intergranular pore size is 50–100 μm, and the intergranular pore size is 30–50 μm for cement or mica filling. The dissolution pores are mainly intragranular pores and intergranular pores. The intergranular pores are mainly kaolinite with small pore size and the maximum pore size is 5 μm (Fig. 1).

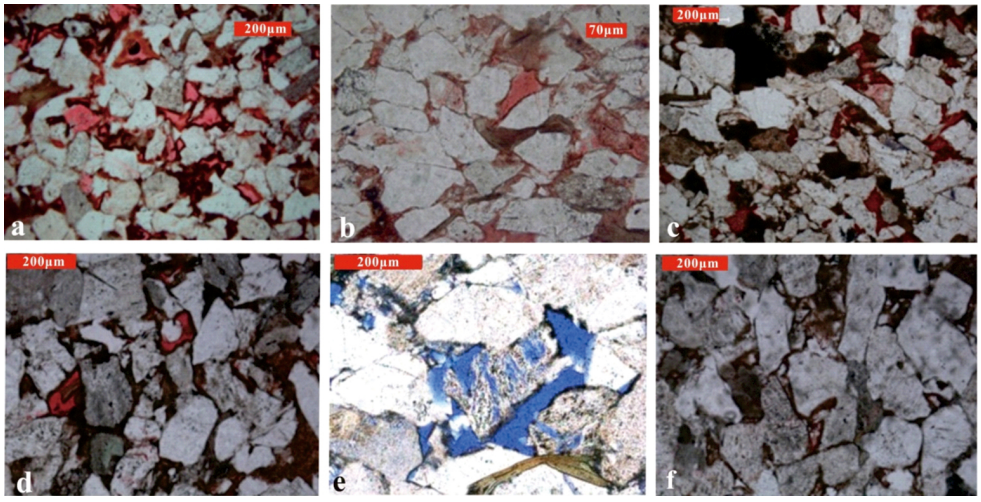

Fig. 1. Reservoir pore characteristics from the Chang 6 member; a) well B209, 1904.9 m, intergranular pore; b) B233, 1931.20 m, intergranular pore-soluble pore; c) D103, 1287.50 m feldspar-debris soluble hole; d) YJ607, primary intergranular pore; e) YJ402, intergranular dissolved pores and feldspar dissolved pores; f) YJ402, intergranular turbid zeolite solution pore

3.2. High pressure mercury injection test results

The mercury injection analysis results of 67 sandstone samples in the Chang 6 member show that the displacement pressure distribution range is 0.28–20.76 MPa, and There is a negative correlation between displacement pressure and permeability; that is, as the sample

permeability increases, the drainage pressure decreases and the sorting performance becomes better. The median pressure distribution range is 0.90–36.88 MPa. Experimental analysis data showed that the maximum distribution range of mercury saturation was 54.5–94.4%, and the mercury removal efficiency distribution range was 13.2–40.6%. There was a large amount of residual mercury in the pores.

By using Washburn equation and capillary pressure curve, the pore throat size distribution of core samples can be quantitatively calculated. From the transformation diagram, it can be directly noted that the pore-throat distribution characteristics of samples with different porosities and permeabilities are also different. Specifically, the peak pore-throat distribution of samples with permeabilities greater than 1.0 mD is greater than 1.0 μm (Fig. 2a). For samples with permeabilities between 0.3 and 1.0 mD, the peak pore-throat distribution was 0.3–1.0 μm (Fig. 2b). For samples with permeabilities between 0.1–0.3 mD, the pore-throat distribution peak was 0.1–0.4 μm, and the main peak distribution was narrow (Fig. 2c). For samples with permeabilities less than 0.1 mD, the peak pore-throat distribution was less than 0.2 μm, and the distribution of the main peak was narrow and showed significant fluctuation (Fig. 2d).

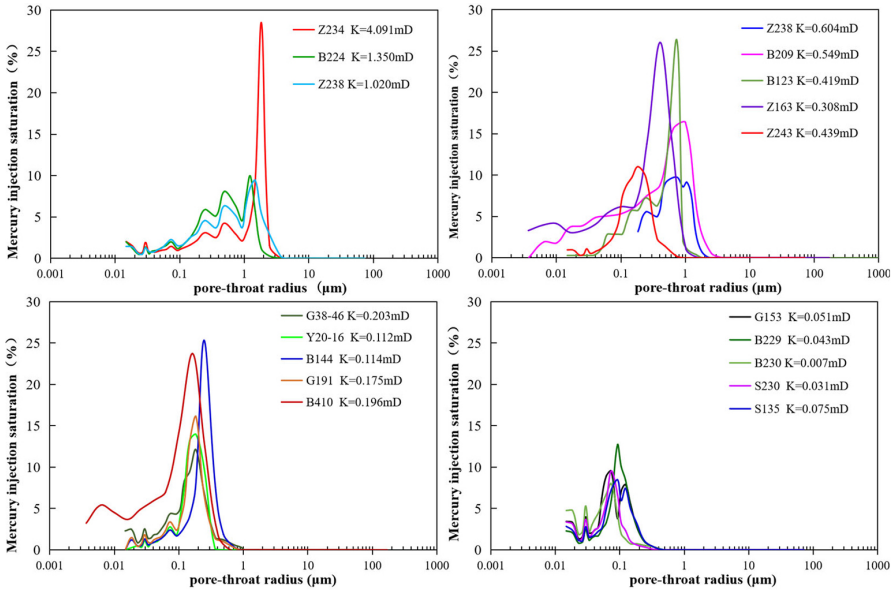

Fig. 2. High pressure mercury injection curves and pore-throat distribution characteristics of the Chang 6 member in the study area

3.3. CT scan results

In this study, micro- and nanometer CT scanning imaging was carried out on the fine sandstone samples from one block in the Chang 6 member. The results show that the Chang 6 member reservoir has a variety of micro- and nanometer-scale pores, which are of various

types and shapes. Comparative qualitative analysis of the two dimensional gray-scale image of the CT scan shows that the main pore type is intergranular, the pore shape is slightly regular, the contact line between pores and particles is relatively straight, and there are no micro-cracks (Fig. 3). The CT scans of the sandstone samples were quantitatively evaluated by a digital core algorithm: The pore coordination number of Chang 6 member was 2–5, with an average of 3. The size distribution of reservoir pore throat was uneven. The pore radius of 85.2% pores was between 20 and 70 μm. The pore radius of 10.4% pores was less than 20 μm. The pore radius of 4.4% pores was greater than 70 μm.

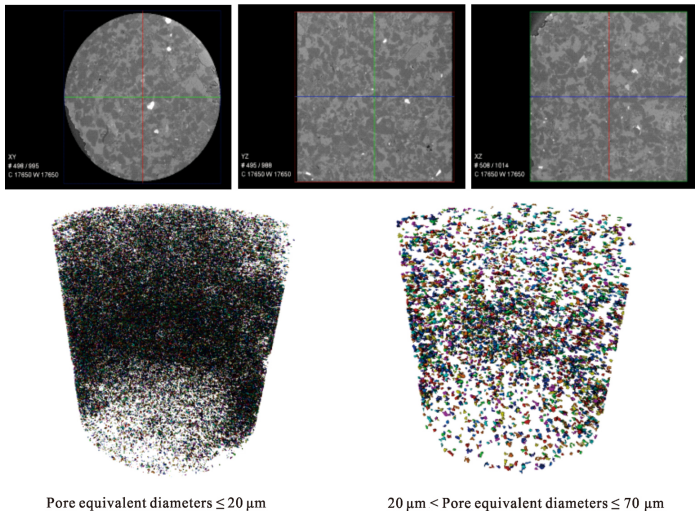

Fig. 3. CT scan characteristics of the sandstone reservoir in the Chang 6 Member in the study area

3.4. Relationship between the pore geometry index (PGI) and porosity and permeability

Porosity is a key parameter to evaluate reservoir property and micro pore structure. Porosity and micro pore structure affect the transfusion characteristics of reservoir. According to the relationship between the PGI and porosity, there is no obvious positive correlation between the porosity and PGI at this location. Pore volume is positively correlated with PGI, that is, PGI increases with the increase of pore volume.

Permeability is the most direct reflection of reservoir permeability, and the micro-pore structure of reservoir directly determines permeability. According to the relationship between the PGI and permeability, there is an obvious observable positive relationship between permeability and the PGI at this site. PGI increases with the increase of permeability. (Fig. 4a).

FZI values are used to evaluate the distribution characteristics of reservoir pore roar from two aspects: porosity and permeability. FZI method is more scientific and reasonable in

reservoir classification. The FZI formula is as follows Eq. (3.1):

$$\text{FZI} = \left(\frac{1-\Phi}{\Phi}\right)\sqrt{\frac{K}{\Phi}} \tag{3.1}$$

In Eq. (3.1), Φ is the porosity, K is the permeability.

There is a piecewise relationship between FZI and PGI. When FZI is less than 25, PGI increases with increasing FZI. When FZI is greater than 25, the PGI decreases with increasing FZI (Fig. 4b). The main reason is that when the porosity of the sample exceeds 12%, permeability increases with abrupt increases in porosity, but for average pore-throat radii and PGI values, the expulsion pressure and comprehensive factors and restraints do not show an obvious relationship.

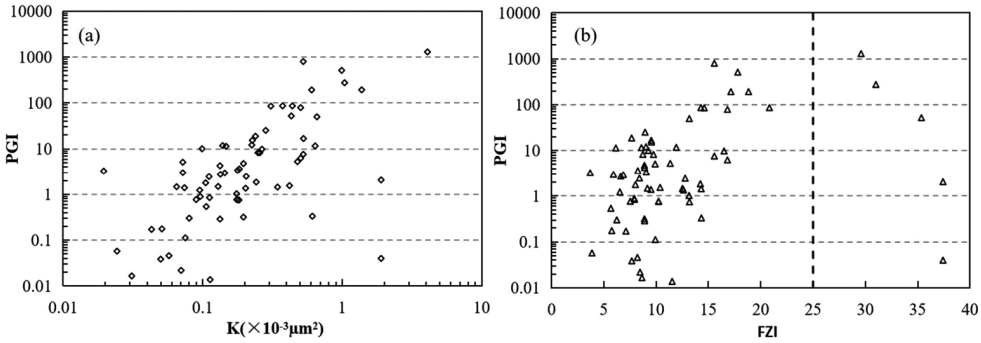

Fig. 4. Relationship between PGI and permeability, FZI

3.5. Relationship between pore geometry index (PGI) and mercury injection parameters

The relationship between the PGI and the displacement pressure can be characterized by an overall power function. The PGI decreases with increasing displacement pressure, and shows a trend of first decreasing quickly, and then decreasing slowly. However, when the displacement pressure is less than 6.75 MPa, the PGI decreases at a faster rate (Fig. 5a).

The relationship between PGI and the maximum pore radius can also be characterized by an overall power function (Fig. 5b). PGI increases with increasing maximum pore radius. However, the test samples are generally divided into two categories, of which the corresponding FZI value of class A is 3.7–37.2, with an average of 11.8. The corresponding FZI values of class B ranged from 3.9 to 37.4, with an average of 12.6. For the samples with discharge pressures greater than 10 MPa, PGI changes very little with increasing discharge pressure.

There was a weak positive correlation between PGI and the maximum mercury injection efficiency overall (Fig. 6a), while there was only a positive correlation between PGI and mercury removal efficiency (Fig. 6b).

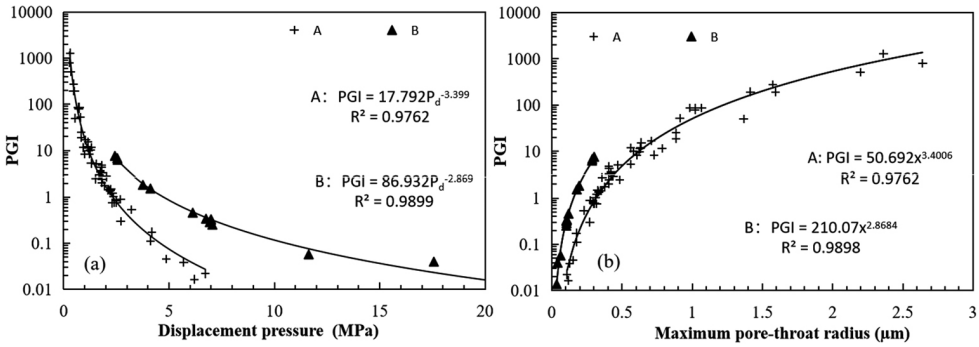

Fig. 5. Relationship between PGI and displacement pressure and maximum pore-throat radius

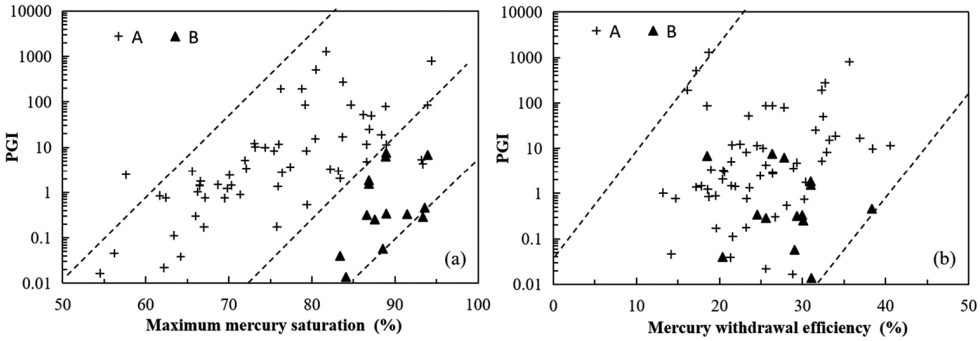

Fig. 6. Relationship between PGI and maximum mercury intake saturation and mercury removal efficiency

4. Response characteristics of logging parameters of different pore structures

Conventional logging data comprehensively reflect the borehole parameters such as the lithology around the borehole, porosity, fluid, drilling fluid and other characteristics of the wellbore and surrounding strata [23]. Multiple regression and neural network methods were comprehensively used to identify and evaluate the pore structure [24].

4.1. Pore structure response in natural gamma logging

In general, the natural gamma value increases with the increase of mud content. Therefore, for the reservoir of Chang 6 member in Baibao area, firstly, the natural gamma curve is used to distinguish sandstone from mudstone; Secondly, the pore structure of the sandstone development section is evaluated; Finally, the evaluation model of pore structure is established with gamma ray logging parameters as input parameters (Fig. 7).

4.2. Pore structure response in spontaneous potential logging

The spontaneous potential curve reflects the permeability of the reservoir. In general, the more permeable the reservoir is, the better the pore structure. For this reason, the relationship $\Delta SP = SP - SSP$ is constructed, where SP is the logging curve value and SSP is the mudstone baseline value. The ΔSP value increases gradually with the change of pore structure from bad to good (Fig. 7).

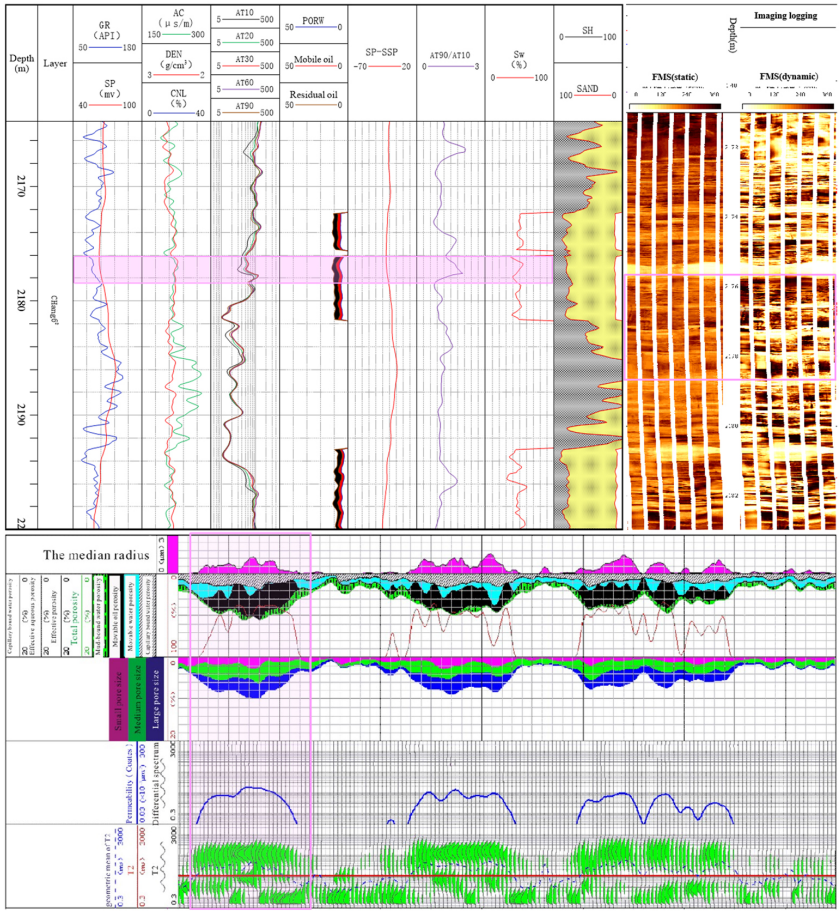

Fig. 7. Logging response characteristics of the pore structure in well G253 (2176.0–2178.5 m)

4.3. Pore structure response to acoustic time

Porosity is one of the key parameters to evaluate pore structure. Acoustic time difference logging is the most commonly used method to calculate reservoir porosity. Usually, acoustic time difference increases with the increase of porosity. Therefore, acoustic time difference logging can be used to evaluate pore structure (Fig. 7).

4.4. Pore structure response to density and compensated neutron logging

Both density logging and compensated neutron logging can be used to calculate reservoir porosity, and the density logging value decreases with increasing porosity. Since compensated neutron logging results increase with porosity, both density and compensated neutron logging can be used to evaluate pore structures (Fig. 7).

4.5. Pore structure response in resistivity logging

In the process of drilling, drilling fluid will permeate along the formation to different degrees. In a sufficiently permeable reservoir development section, there is a certain amplitude difference between the deep resistivity, medium resistivity and shallow resistivity logging curve values. Generally, the better the permeability the reservoir is, the more obvious the amplitude difference (Fig. 7). The depth resistivity ratio (RILD/RILM) parameter was constructed to evaluate the reservoir pore structure.

4.6. Pore structure response of FMI and NMR

The imaging results of the logs show that the reservoir with moderate to good pore structure has bright block characteristics and relatively well developed pores. In reservoirs with poor pore structures, the imaging logs generally show banded, speckled or dark characteristics. NMR logging can directly reflect the proportion of large pores, medium pores and small pores in the reservoir, which is widely used in the development of tight sandstone reservoir, shale oil and shale gas. Taking 2176.0–2178.5 m in well G253 as an example (Fig. 7), the average natural gamma ray is 79.8 API, the average acoustic time difference is 238.4 μs/m, and the density is 2.52 g/cm^3. The resistivity results of the deep and shallow induction logging have obvious amplitude differences. In NMR logging, the total porosity of the formation is 12.63%, the effective pore volume is 8.62%, the movable fluid volume is 6.19%, and the capillary bound water volume is 2.44%. The results show that the pore size of small pore size, medium pore size and large pore size are 1.41%, 3.24% and 3.39%, respectively, the permeability is 1.16×10^{-3} μm^2 and the water saturation is 43%. The pore volumes of the large and medium pore sizes are similar and represent a high proportion of the pores, while the pore volume of small pore sizes is minimal. According to the imaging logging results, the lithology of this section is uniform, with good physical properties and pore structure.

5. Pore structure logging evaluation model

5.1. Multiple parameter statistical method

Based on the analysis results, such as from the high pressure mercury injection and thin section analysis, the pore structure from 67 samples of the Chang 6 member was combined with logging response parameters to establish the correlation between natural gamma rays, acoustic time differences, compensating neutrons, resistivity, density, spontaneous potential

and pore structure (Fig. 8). The results show that in logarithmic coordinates, natural gamma rays, deep induction resistivity and acoustic time difference and the PGI were positively related and negatively correlated with the density parameter. Then, the logging parameters and PGI of the quantitative evaluation model were established (Table 1). The five parameter model had the highest correlation and was chosen to calculate the PGI and the mercury injection experiment data was used to calculate the PGI contrast display (Fig. 9). The correlation coefficient R^2 was 0.9086, and the average relative error was 8.4%.

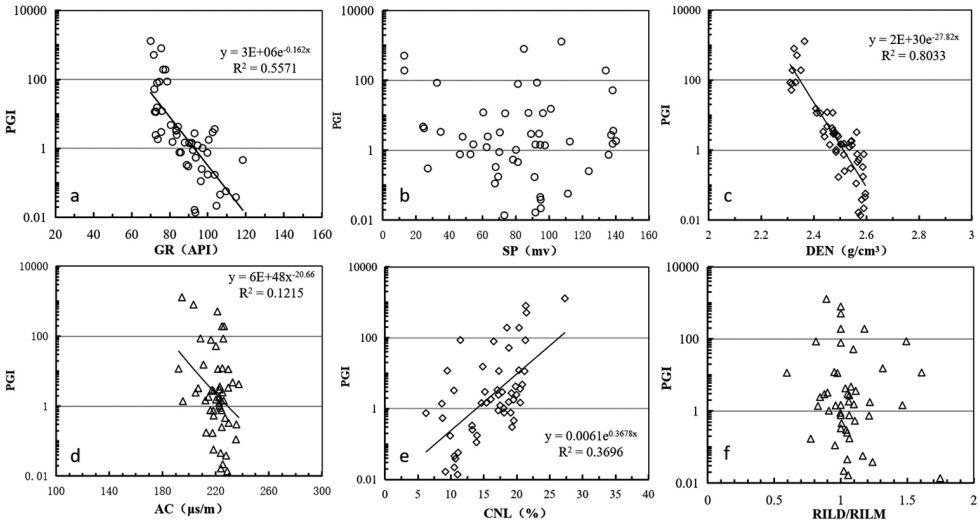

Fig. 8. Exponential relationship between logging parameters and pore structure

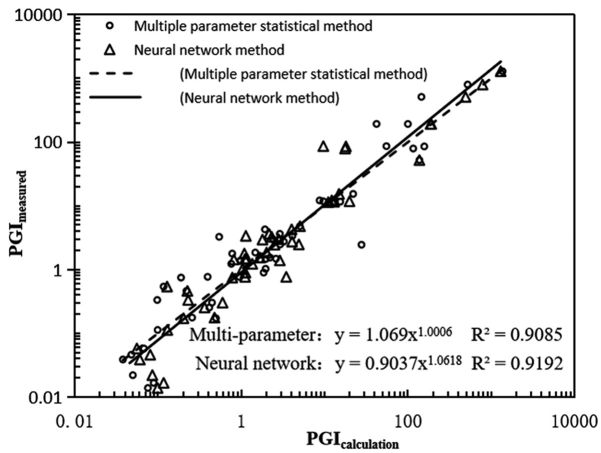

Fig. 9. Comparison of the measured pore geometry index (PGI) and modelled PGI

Table 1. Multiparameter statistical evaluation of the pore structure model

Number of parameters	Model formula	R^2
Double	LN(PGI) = −0.052 · GR − 22.675 · DEN + 6.670	0.83
Three	LN(PGI) = −0.028 · GR − 0.068 · AC − 19.232 · DEN + 63.317	0.86
Four	LN(PGI) = −0.028·GR−0.068·AC−19.232·DEN+0.169·CNL+63.317	0.90
Five	LN(PGI) = −0.028 · GR − 0.069 · AC − 19.268 · DEN + 0.168 · CNL − 0.006 · (RILD/RILM) + 63.608	0.91

5.2. Neural network method

BP neural network algorithm is a method of machine learning, which has great advantages in the simulation of nonlinear relationship research [25]. The relationship between the porosity and permeability parameters of tight sandstone reservoir and the value of logging curve is not linear. BP method can effectively solve this complex nonlinear problem, and achieve good application effect in the development and utilization of tight oil, shale gas and shale oil.

In this study, using the PGI quantitative characterizations of the pore structure, we analyze the different logging response characteristics of the curve according to the PGI. We then select the natural gamma ray, acoustic time, compensated neutron, density, deep resistivity and shallow resistivity, natural potential difference value from seven logging parameters as the input layer, and configure two hidden layers. The PGI is taken as the output layer. The results show that the correlation coefficient (R^2) between the PGI analyzed by the experiment and the PGI predicted by the model is 0.9192, and the relative error is 7.9% on average (Fig. 9).

5.3. The example analysis

Taking the 2049.34–2057.62 m section of well G255 as an example (Fig. 10), the multiparameter regression method and neural network method were used to calculate the PGI. The results show that the PGI calculated by the multiparameter regression method is 4.52–15.08, with an average of 9.48. The PGI calculated by the neural network method is 1.22–13.83, which reflects the pore structure of the section is good. The NMR data show that the effective pore volume is 7.58%, the small pore volume is 0.93%, the medium pore volume is 3.5%, and the large pore size is 3.20%, reflecting the pore structure of the section is good. This shows that it is feasible to reliably calculate the PGI with conventional logging parameters.

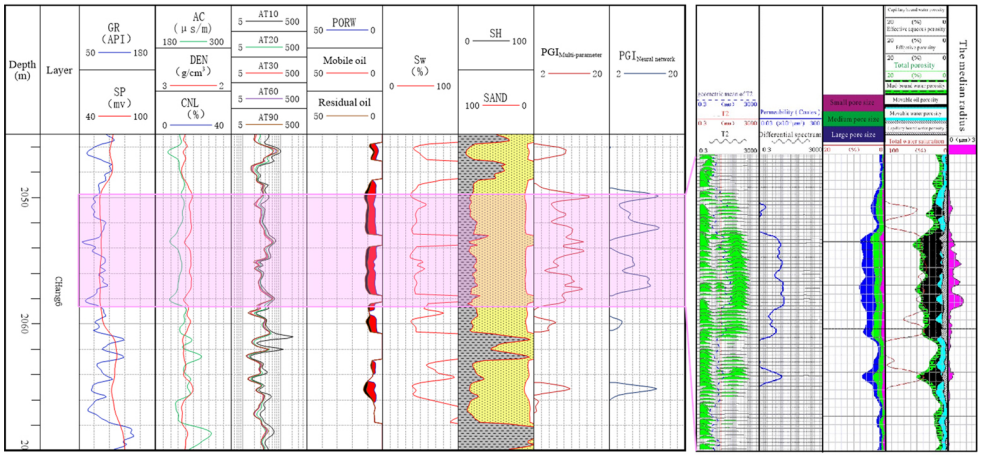

Fig. 10. Prediction results of the pore geometry index

6. Conclusions

1. The Chang 6 Member reservoir in Baibao area is a typical low porosity and low permeability reservoir. There are various pore types, such as intergranular pore, dissolution pore and intergranular pore. The pore radius is mainly 20–70 μm, and the volatility of the curve is obviously enhanced.
2. In tight sandstone reservoirs, PGI can effectively characterize pore structure. Among the pore structure parameters, the maximum pore throat radius, displacement pressure and FZI are closely related to PGI, and the PGI model of each parameter is established.
3. Gamma ray, natural potential separation, acoustic time, density, compensated neutron, deep resistivity, and shallow resistivity logs all reflect the attributes of reservoir pore structure. Logging a single parameter to evaluate reservoir pore structure has certain limitations. However, multiparameter regression and neural networks can be used to apply pluralistic and nonlinear methods to quantitatively evaluate pore structure. Furthermore, neural network prediction accuracy is higher that predictions made from other methods.
4. The neural network method and multiple parameter regression were used to evaluate the pore structure of the reservoir. From these results, the continuous and quantitative PGI was calculated from a single well. This approach could be applied in untapped wells and could be used as one of the parameters considered to evaluate the pore structure of the reservoir.

Acknowledgements

The authors wish to thank The Doctoral Start-up Fund Project of Yan'an University (Project Number: YUA202213123), the Science and Technology Plan Project of Yan'an City (Project Number: 2023-GYGG-009), the Young Talent Fund of Association for Science and Technology in Shaanxi, China (Project Number: 20220459), the Science and Technology Plan Project of Yulin City (Project Number: CXY-2022-184).

References

[1] G.R. Zhong, "Optimization of logging saturation interpretation model under the constraint of reservoir conditions-A case study of the Chang 6 member Yanchang Formation in the central Ordos Basin", Xi'an: Northwest University, 2022, doi: 10.27405/d.cnki.gxbdu.2022.001134.

[2] R. Zhu, S. Wu, L. Su, J. Cui, Z. Mao, and X. Zhang, "Problems and future works of porous texture characterization of tight reservoirs in China", *Acta Petrolei Sinica*, vol. 37, no. 11, pp. 1323–1336, 2016, doi: 10.7623/syxb201611001.

[3] S. Wu, R. Zhu, J. Cui, Z. Mao, K. Liu, and X. Wang, "Ideas and prospect of porousstructure characterization in unconventional reservoirs", *Geological Review*, vol. 66, supp1, pp. 151–154, 2020, doi: 10.16509/j.georeview.2020.s1.058.

[4] Y. Xue, J. Liu, P. G. Ranjith, F. Gao, H. Xie, and J. Wang, "Changes in microstructure and mechanical properties of low-permeability coal induced by pulsating nitrogen fatigue fracturing tests", *Rock Mechanics and Rock Engineering*, vol. 55, pp. 7469–7488, 2022, doi: 10.1007/s00603-022-03031-2.

[5] J.M. Davis, N.D. Roy, P.S. Mozley, and J.S. Hall, "The effect of carbonate cementation on permeability heterogeneity in fluvial aquifers: An outcrop analog study", *Sedimentary Geology*, vol. 184, no. 3-4, pp. 267–280, 2006, doi: 10.1016/j.sedgeo.2005.11.005.

[6] T.T. Eaton, "On the importance of geological heterogeneity for flow simulation", *Sedimentary Geology*, vol. 184, no. 3-4, pp. 187–201, 2006, doi: 10.1016/j.sedgeo.2005.11.002.

[7] Y. Zhao, M. Zhao, Y. Zhao, B. Wang, and B. Cao, "A new appoach of analyzing digital image of pore system of carbonate rocks", *Natural Gas Industry*, vol. 26, no. 12, pp. 75–78, 2006.

[8] B.B. Bowen, B.A. Martini, M.A. Chan, and W.T. Parry, "Reflectance spectroscopic mapping of diagenetic heterogeneities and fluid-flow pathways in the Jurassic Navajo Sandstone", *AAPG Bulletin*, vol. 91, no. 2, pp. 173–190, 2007, doi: 10.1306/08220605175.

[9] P. Németh, M. Tribaudino, E. Bruno, and P.R. Buseck, "TEM investigation of Ca-rich plagioclase: Structural β uctuations related to the I1-P1phase transition", *American Mineralogist*, vol. 92, no. 7, pp. 1080–1086, 2007, doi: 10.2138/am.2007.2504.

[10] J. Mayer, L.A. Giannuzzi, T. Kamino, and M. Joseph, "TEM sample prepara-tion and FIB-induced damage", *MRS Bulletin*, vol. 32, no. 5, pp. 400–407, 2007, doi: 10.1557/mrs2007.63.

[11] H. Wu, C. Zhang, Y. Ji, R. Liu, S. Cao, S. Chen, Y. Zhang, Y. Wang, W. Du, and G. Liu, "Pore throat size characterization of tight sandstons and its cantrol on reservoir physical properties: A case study of YanChang Formation, eastern Gansu, Ordos Basin", *Acta Petrolei Sinica*, vol. 38, no. 8, pp. 876–887, 2017, doi: 10.7623/syxb201708003.

[12] A.P. Radlinski, M. Mastalerz, A.L. Hinde, M. Hainbuchneer, H. Rauch, M. Baron, J. Lin, L. Fan, and P. Thiyagarajan, "Application of SAXS and SANS in evaluation of porosity, pore size distributionand surface area of coal", *International Journal of Coal Geology*, vol. 59, no. 3/4, pp. 245–271, 2004, doi: 10.1016/j.coal.2004.03.002.

[13] Y.B. Melnichenko, A.P. Radlinski, M. Mastalerz, G. Cheng, and J. Rupp, "Characterization of the CO2 fluid adsorption in coal as a function of pressure using neutron scattering techniques (SANS and USANS)", *International Journal of Coal Geology*, vol. 77, no. 1/2, pp. 69–79, 2009, doi: 10.1016/j.coal.2008.09.017.

[14] J. Bahadur, Y.B. Melnichenko, M. Mastalerz, A. Furmann, and C.R. Clarkson, "Hierarchical pore morphology of Cretaceous shale: A small-angle neutron scatteringand ultrasmall-angle neutron scattering study", *Energy and Fuels*, vol. 28, no. 10, pp. 6336–6344, 2014, doi: 10.1021/ef501832k.

[15] A.A. Hinai, R. Rezaee, L. Esteban, and M. Labani, "Comparisons of pore size distribution: A case from the Western Australian gas shale formations", *Journal of Unconventional Oil and Gas Resources*, vol. 8, pp. 1–13, 2014, doi: 10.1016/j.juogr.2014.06.002.

[16] J.J. Cao, C.B. Chen, J.L. Luo, and X. Wang, "Impact of authigenic clay minerals on micro-heterogeneity of deep water tight sandstone reservoirs: a case study of Triassic Chang 6 oil reservoir in Heshui area, southwestern Ordos Basin", *Lithologic Reservoirs*, vol. 32, no. 6, pp. 36–49, 2020, doi: 10.12108/yxyqc.20200604.

[17] X. Wu, L. Ji, W. Wu, F. Li, L. Zeng, C. Duan, H. Wei, and Y. Li, "Classification and characterization of low permeability sandstone reservoir based on complex pore structure analysis", *Journal of Northwest University (Natural Science Edition)*, vol. 50, no. 4, pp. 615–628, 2020, doi: 10.16152/j.cnki.xdxbzr.2020-04-013.

[18] J. Zhang, H. Liu, and W. Liu, "Application of NMR data to evaluation of deep glutenite pore structure and reservoir validity", *Well Logging Technology*, vol. 6, no. 3, pp. 256–260, 2012, doi: 10.16489/j.issn.1004-1338.2012.03.009.

[19] T. Zhang, X.G. Zhang, C.Y. Lin, and C. Dong, "Evaluation of pore structure in low permeability reservoirs based on common well logs", *Journal of Chengdu University of Technology (Science & Technology Edition)*, vol. 41, no. 4, pp. 413–421, 2014, doi: 10.3969/j.issn.1671-9727.2014.04.02.

[20] Y. Xue, P.G. Ranjith, Y. Chen, C. Cai, F. Gao, and X. Liu, "Nonlinear mechanical characteristics and damage constitutive model of coal under CO_2 adsorption during geological sequestration", *Fuel*, vol. 331, art. no. 125690, 2023, doi: 10.1016/j.fuel.2022.125690.

[21] X. Zhao, B. Liu, R. Guo, D. Zhang, Y. Li, and Z. Tian, "Reservoir characterization and its application to development", *Petroleum Geology and Experiment*, vol. 39, no. 2, pp. 287–294, 2017, doi: 10.11781/sysydz201702287.

[22] T. Zhang and P. Hao, "Fine charactization of the reservoir space in deep ultra-low porosity and ultra-low permeability glutenite in Bozhong Sag", *Bulletin of Geological Science and Technology*, vol. 39, no. 4, pp. 117–124, 2020, doi: 10.19509/j.cnki.dzkq.2020.0415.

[23] G.R. Zhong, X.L. Zhang, Z. Yang, J. Lu, X. Zhao, and X. Wang, "Logging identification method for fractures in tight sandstone reservoirs of Yanchang Formation in Dingbian-Zhidan area, Ordos Basin", *Progress in Geophysics*, vol. 36, no. 4, pp. 1669–1675, 2021, doi: 10.6038/pg2021EE0318.

[24] T. Godlewski, E. Koda, M. Mitew-Czajewska, S. Łukasik, and S. Rabarijoely, "Essential georisk factors in the assessment of the influence of underground structures on neighboring facilities", *Archives of Civil Engineering,* vol. 69, no. 3, pp. 113–128, 2023, doi: 10.24425/ace.2023.146070.

[25] Z.H. Zhang, J.B. Liao, Z.Y. Li, X.M. Zheng, J. Di, and P. Yu, "Fast prediction of productivity level of low permeability reserviors based on multilayer perceptron: a case study of Chang3,4+5 reservoirs of Baibao-Nanliang area in Ordos basion", *Progress in Geophysics*, vol. 34, no. 5, pp. 1962–1970, 2019, doi: 10.6038/pg2019CC0417.

Received: 2023-10-25, Revised: 2024-01-23